NONLINEAR HYBRID MODEL OF SINGLE PROTECTION VALVE FOR PNEUMATIC BRAKE SYSTEMS

H. Németh – P. Ailer – K. M. Hangos

SCL-002/2002

(Research report)

May 2002

ABSTRACT

This paper is motivated by the fact that application of protection valves in conventional air brake systems is common and new generation air supply systems with integrated electronic control will use this onward with slight modifications. So its dynamic behaviour and properties are essential for designing such a system. The objective of this paper is to build up an engineering index-1 hybrid model in DAE form of a single protection valve with electronic actuation for control design purpose including the model verification.

CONTENTS

1 INTRODUCTION

From the view of air conservation commercial vehicle air brake systems can be divided into three main hierarchical parts: air supply-, air treatment- and air consumption subsystem.

The air supply part has only one member: the compressor (3 in Fig.1). The air consumption part has several members carrying out the control of brake chamber pressure to satisfy the driver's deceleration demand. Furthermore, air spring and some auxiliary systems (e.g. boosters) belong to the air consumption subsystem, too.

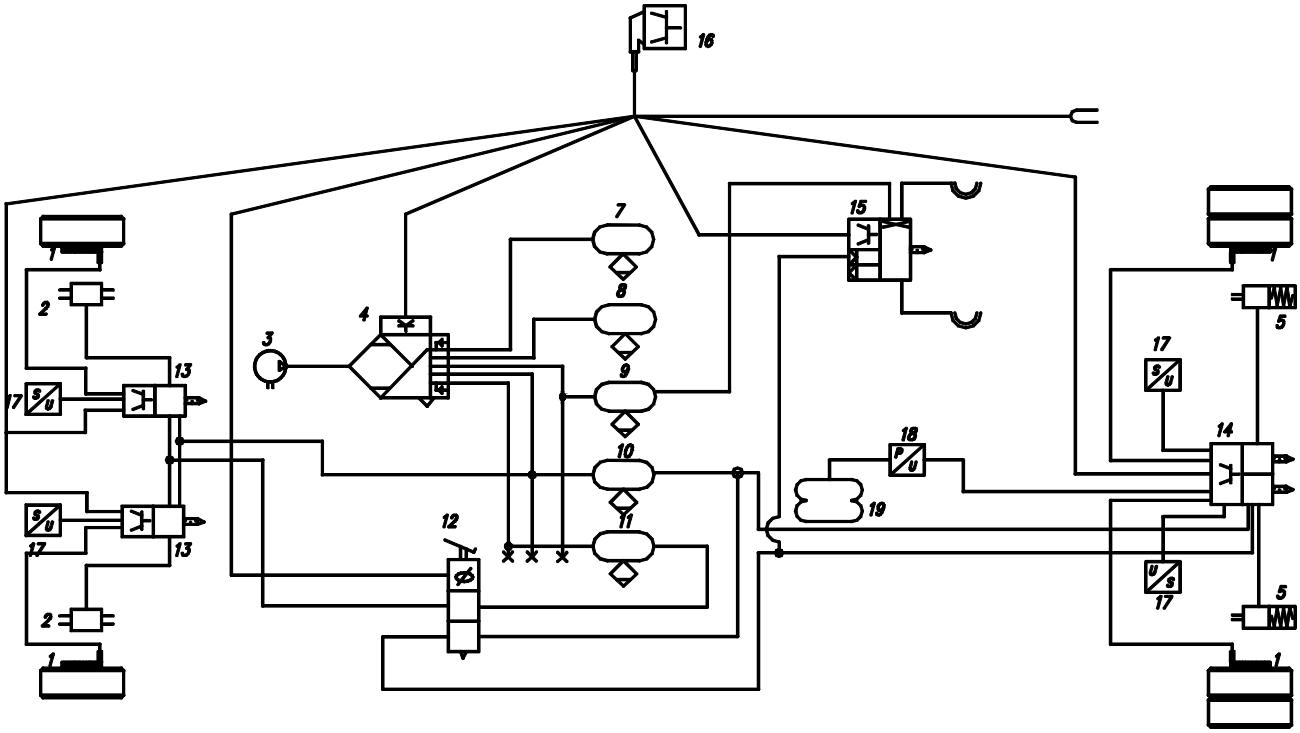

Figure 1 Layout of electro-pneumatic brake system with electronic air treatment of a towing vehicle (4x2)

Air treatment systems, being in the focus of this paper, consist of three main functional parts: system pressure control, air-drying (4) equipped with integrated system pressure control valve and air distribution into circuits. This last component usually consists of different number of protection valves, which ensure the independence and safety of circuits, as well as they set up the circuit fill up sequence. The number of these valve elements is the same as the number of independent circuits. This is typically four, but there are signs, which indicate that this will be increased in the future.

Sometimes multi-circuit protection valves include integrated pressure limiters, too, to carry out multipressure compressed air system.

The single protection valve (see Fig.2) consists of the valve housing (6) with seat (5), gasket plate (4), piston (1) and preset spring (2). The opening orifice is determined by the seat edge (3). Input connection is denoted as C1, output connection as C2.

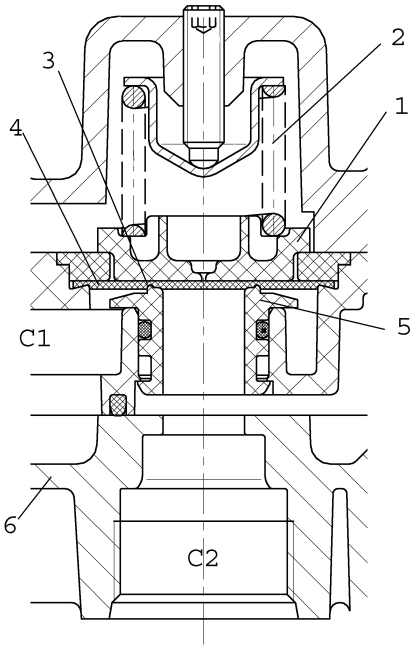

Figure 2 Single protection valve in a valve unit

2 MODEL OF PROTECTION VALVE

2.1 PROBLEM SETUP

In future air treatment systems protection valves will be equipped with electronic pressure limiting (avoiding pneumatic limiter – cost reduction). This can be achieved by controlling the chamber pressure over the piston part (1 in Fig.2). To develop the proper controller it is required to build up the model of this dynamic system [1], [2]. Considering that the pressure limiting is controlled at a sampling frequency in the order of magnitude of 100 Hz [9], dynamic behaviour of the pneumatic components must be taken into account in design of electronic air supply system composition and control if appropriate circuit fill operation is to be guaranteed, especially having no reservoir in the corresponding circuit [4], [8].

2.2 SYSTEM DESCRIPTION

The system to be modelled consists of the following elements, which are relevant in the protection valve's operation (see Fig. 3):

- **Input chamber** with volume of V_1 (1) This chamber has an input (air flow from compressor) and an output towards the protection valve.
- **Input piping** (2)

- **Protection valve** (3) The valve has an input connection from the input chamber through the input pipe and an output to the output chamber (circle reservoir)
- **Output piping** (4)
- **Output chamber** with volume of V_2 (5) This chamber has an input from protection valve and an output towards the brake system or other consumers.
- **Control chamber** with volume of V_3 (6) This chamber has a supply from the input chamber and an output towards the magnet valve.
- **Control magnet valve** (7)

Input chamber models mainly the piping volume between the compressor and the protection valve, output chamber serves as the effective reservoir of the circuit.

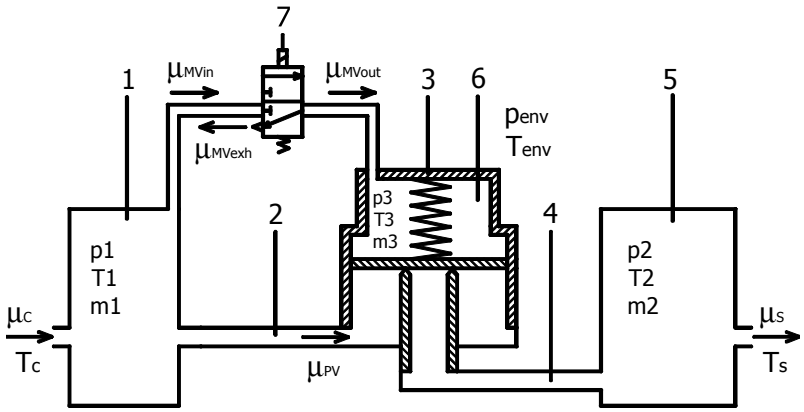

Figure 3 Base model of single protection valve

Control aim

The following control aim is considered:

- The circuit pressure has to be limited according to a target pressure; it should be within a given range and should not be disturbed by compressor performance and circuit air consumption, circuit volume V_2.
- The control has to be robust concerning the disturbances and the parameters of the linearized model

2.3 MODELLING ASSUMPTIONS

When constructing the model of the simplified system, shown in Fig. 3, the following assumptions have been made:

General assumptions

- The gas physical properties are assumed to be constant over the whole time and temperature domain such as specific heats, gas constant and adiabatic exponent.

- All chamber pressures are higher or equal to the environment pressure
- The gas physics in the cambers are perfectly mixed

Other assumptions:

- The magnet valve elements were modelled as magneto-dynamically homogeneous material.
- Compressor airflow is assumed to have non-negative values only; all other airflows can have negative and positive values, too.
- Magnet valve body maximal stroke, inlet and exhaust port diameters are assumed to satisfy that: $x_{MV\max} > \frac{d_{MVin}}{4} + \frac{d_{MVexh}}{4}$
- Magnet valve port cross sections are assumed to satisfy that: $A_{MVout} >> A_{MVin}, A_{MVexh}$

2.4 MODEL ACCURRACY

The resulted model should describe the dynamic behaviour of the real process within 10% desired accuracy [3].

3 HYBRID BEHAVIOUR

The system contains many subsystems that exhibit non-continuous or non-smooth behaviour. This means that the equations, which describe the dynamic behaviour of the corresponding subsystem varies according to some circumstances [3]. The method for constructing a hybrid model capable of describing such behaviour is to define first the state equations or conservation equations and the consecutive or algebraic equations for a given set of states (one state for each hybrid component) then we investigate these hybrid subsystems in each state to generalize the model and to form a composite hybrid model there from.

This investigated special hybrid state is basically the fill up procedure of outlet chamber (brake circuit) filling the inlet chamber by the compressor without excited magnet valve, where the streaming process is subsonic. By analysing each subcomponent that refer to this hybrid state this means:

- The compressor is in charge phase; the protection valve is in opening situation and has positive value airflow. This charges the outlet chamber. The magnet valve is not excited so its inlet airflow is zero. It corresponds to Inlet chamber Hybrid-state 1 in chapter 6.1.1.

- The positive value airflow of the protection valve charges the outlet chamber where the airflow into the brake system is non-negative. It corresponds to Outlet chamber Hybrid-state 1 in chapter 6.1.2.
- Since the magnet valve is not excited it exhausts the control chamber of the protection valve. This corresponds to Control chamber Hybrid-state 1 in chapter 6.1.3.
- The protection valve is open and so the stroke does not exceed the limits and the determinant streaming cross section is a cylinder surface. It corresponds to Protection valve streaming cross section Hybrid-state 2 in chapter 6.2.1 and Protection valve limiting force Hybrid-state 2 in 6.3.1.
- The magnet valve is not excited and it is in its standstill stroke. It corresponds to Magnet valve streaming cross section Hybrid-state 4 in chapter 6.2.2 and Magnet valve limiting force Hybrid-state 2 in chapter 6.3.2.
- The stream through the protection valve is considered subsonic. It corresponds to Protection valve airflow Hybrid-state 1 in chapter 6.4.1.
- Since the magnet valve is not excited and its inlet port is closed so the inlet stream of the magnet valve is zero. It corresponds to Magnet valve inlet airflow Hybrid-state 1 in chapter 6.4.2.1.
- The exhaust stream of the magnet valve is considered subsonic and exhausting the control chamber. It corresponds to Magnet valve exhaust airflow Hybrid-state 1 in chapter 6.4.2.2.

4 STATE EQUATIONS

The model equations are developed from conservation balances. There are gas mass balance, internal gas energy, mechanical energy and electro-magnetic energy conservation laws that have to be used [5], [7], [9]. The table of notation can be found in the Appendix.

4.1 CONSERVATION LAWS OF GAS MASS BALANCE

The gas mass balances of the chambers can be written as:

$$\frac{dm_1}{dt} = \mu_C - \mu_{PV} - \mu_{MVin}, \tag{1}$$

$$\frac{dm_2}{dt} = \mu_{PV} - \mu_S, \tag{2}$$

$$\frac{dm_3}{dt} = \mu_{MVout}. \tag{3}$$

4.2 CONSERVATION LAWS OF GAS INTERNAL ENERGY BALANCE

The internal energy balance of the cambers can be denoted as follows:

$$\frac{dU_1}{dt} = \mu_C i_1 - \mu_{PV} i_v - \mu_{MVin} i_3 + Q_1, \tag{4}$$

$$\frac{dU_2}{dt} = \mu_{PV} i_v - \mu_S i_2 + Q_2, \tag{5}$$

$$\frac{dU_3}{dt} = \mu_{MVout} i_3 + Q_3. \tag{6}$$

The expanded internal energy equations are as (considering air flow directions as shown in Fig.3):

$$\frac{dU_1}{dt} = c_p\left(\mu_C T_C - \mu_{PV} T_1 - \mu_{MVin} T_1\right) - k_1 A_1\left(T_1 - T_{env}\right), \tag{7}$$

$$\frac{dU_2}{dt} = c_p\left(\mu_{PV} T_1 - \mu_S T_2\right) - k_2 A_2\left(T_2 - T_{env}\right), \tag{8}$$

$$\frac{dU_3}{dt} = c_p \mu_{MVout} T_1 - k_3 A_3\left(T_3 - T_{env}\right). \tag{9}$$

The state equation for chamber gas temperatures can be obtained from the internal energy as:

$$\frac{dU}{dt} = \frac{d\left(c_v m T\right)}{dt} = c_v T \frac{dm}{dt} + c_v m \frac{dT}{dt}, \tag{10}$$

The derived state equation for gas temperatures from equations (7), (8), (9) and (10) are as follows:

$$\frac{dT_1}{dt} = \kappa \frac{\mu_C T_C - \mu_{PV} T_1 - \mu_{MVin} T_1}{m_1} - \frac{k_1 A_1\left(T_1 - T_{env}\right)}{c_v m_1} - \frac{T_1}{m_1}\left(\mu_C - \mu_{PV} - \mu_{MVin}\right), \tag{11}$$

$$\frac{dT_2}{dt} = \kappa \frac{\mu_{PV} T_1 - \mu_S T_2}{m_2} - \frac{k_2 A_2\left(T_2 - T_{env}\right)}{c_v m_2} - \frac{T_2}{m_2}\left(\mu_{PV} - \mu_S\right). \tag{12}$$

$$\frac{dT_3}{dt} = \kappa \frac{\mu_{MVout} T_1}{m_3} - \frac{k_3 A_3\left(T_3 - T_{env}\right)}{c_v m_3} - \frac{T_3}{m_3}\mu_{MVout}. \tag{13}$$

where

$$\kappa = \frac{c_p}{c_v}. \tag{14}$$

4.3 DYNAMIC EQUATIONS OF THE PROTECTION VALVE PISTON

Newton's second law has been used for constructing the dynamic equations of the protection valve piston:

$$\frac{d^2 x_{PV}}{dt^2} = \frac{F_{PV1} + F_{PV2} - c_{PV}\left(x_{PV} + x_{0PV}\right) - k_{PV}\dot{x}_{PV} - p_3 \frac{d_1^{\,2}}{4}\pi + F_{PV\,\lim}}{m_{PV}}, \tag{15}$$

where F_1 is the force acting on the donut surface and F_2 is on the inner circular surface and $F_{\lim}$ is the force limiting the stroke in each directions. In order to transform the above equation to its state equation form two first order equations are used instead of the second order one (15), so:

$$\frac{dx_{PV}}{dt} = v_{PV}, \tag{16}$$

and

$$\frac{dv_{PV}}{dt} = \frac{F_{PV1} + F_{PV2} - c_{PV}\left(x_{PV} + x_{0PV}\right) - k_{PV} v_{PV} - p_3 \frac{d_1^{\,2}}{4}\pi + F_{PV\lim}}{m_{PV}}. \tag{17}$$

Similarly Newton's second law has been used for the balance of magnet valve body as:

$$\frac{d^2 x_{MV}}{dt^2} = \frac{F_{MV} - c_{MV}\left(x_{MV} + x_{0MV}\right) - k_{MV}\dot{x}_{MV} + F_{MV\lim}}{m_{MV}} \tag{18}$$

The two first order equations can be derived as:

$$\frac{dx_{MV}}{dt} = v_{MV}, \tag{19}$$

and

$$\frac{dv_{MV}}{dt} = \frac{F_{MV} - c_{MV}\left(x_{MV} + x_{0MV}\right) - k_{MV} v_{MV} + F_{MV\lim}}{m_{MV}} \tag{20}$$

4.4 ELECTRO-MAGNETIC CONSERVATION

The relationship between voltage and current is as follows:

$$U = R\,I + L\frac{dI}{dt} + I\frac{dL}{dt}, \tag{21}$$

where U is the input voltage, R denotes the ohmic resistance. The inductance of the solenoid can be written as:

$$L = \frac{N^2}{R_\Sigma}. \tag{22}$$

In the above equation N is the number of solenoid turns and R_Σ is the valve position-dependent magnetic resistance. In (21) $\frac{dL}{dt}$ can be expressed as $\frac{dL}{dx_{MV}}\frac{dx_{MV}}{dt}$ and $\frac{dL}{dx_{MV}}$ can be written as $\frac{dL}{dR_\Sigma}\frac{dR_\Sigma}{dx_{MV}}$ so the equation can be rewritten in state variable form as:

$$\frac{dI}{dt} = \frac{U}{L} - \frac{R\,I}{L} + \frac{I}{L}\frac{dL}{dR_\Sigma}\frac{dR_\Sigma}{dx_{MV}} v_{MV}. \tag{23}$$

In conclusion: the first order state equations of the single protection valve consists of the equations (1), (2), (3), (11), (12), (13), (16), (17), (19), (20) and (23). The number of state equations is considered too high for controller design, which requires a model simplification before that.

5 CONSTITUTIVE EQUATIONS

These equations are needed to define transfer rates, property relations, equipment constraints and other characterizing variables.

5.1 BALANCE OF THE PROTECTION VALVE PISTON

On the upper side the piston is affected by a cylindrical spring and the control pressure (p_3). On the lower side it is affected by the pressure distribution in the inner circular section (output side - p_2) and outer donut section (input side - p_1).

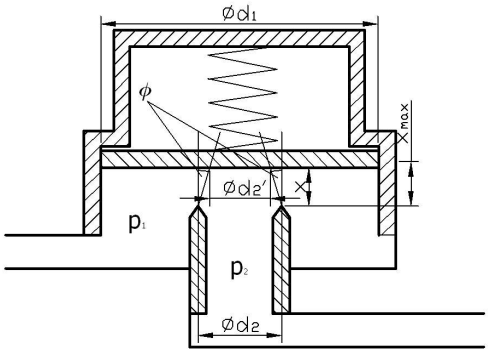

Figure 4 Model for piston balance

To evaluate the delimitation between input and output pressures a cone model is used with varying pitch angle (φ). The cross section of this cone and the piston determines the border between input and output side pressure surfaces (see Fig. 4).

The pitch angle varies as follows: if c velocity is positive (circuit fill situation) the effected inner radius of the donut is decreased ($\varphi > 0$) because the pressure distribution inherits on this surface mainly the input side pressure. The inner circular section's radius is also decreased by this change.

If c is negative ($\varphi < 0$) the donut surface decreases, the circular one increases. This radius change is determined by the angle of the ray line (pitch-cone), which is searched as function of the local speed at the critical section:

$$\varphi = f(s_{PV}) \tag{24}$$

The relationship is searched in the following linearized form:

$$\varphi = a_1 + a_2 s_{PV}, \tag{25}$$

where c is the air speed at *vena contracta.* Force acting on the donut surface can be written as:

$$F_{PV1} = p_1 \left(\frac{{d_1}^2}{4} - \frac{\left(d_2 - 2x\,tg(\varphi)\right)^2}{4} \right) \pi \,, \tag{26}$$

F_2 is on the inner circular surface (determined by d_2'):

$$F_{PV2} = p_2 \frac{\left(d_2 - 2x\,tg(\varphi)\right)^2}{4} \pi \,. \tag{27}$$

The stroke limiting force is:

$$F_{PV\,\lim} = 0 \tag{28}$$

5.2 AIRFLOW PROPERTIES OF THE PROTECTION VALVE

Streaming cross section of protection valve can be calculated as:

$$A_{PV} = x d_2 \pi \tag{29}$$

The local gas speed in protection valve at *vena contracta*:

$$s_{PV} = \sqrt{2 \frac{\kappa}{\kappa - 1} R T_1 \left[1 - \left(\frac{p_2}{p_1} \right)^{\frac{\kappa - 1}{\kappa}} \right]} \,, \tag{30}$$

The mass flow through the protection valve is written as:

$$\mu_{PV} = \alpha_{PV} A_{PV} \sqrt{2 \frac{\kappa}{\kappa - 1} \frac{p_1 m_1}{V_1} \left[\left(\frac{p_2}{p_1} \right)^{\frac{2}{\kappa}} - \left(\frac{p_2}{p_1} \right)^{\frac{\kappa + 1}{\kappa}} \right]} \tag{31}$$

Chamber pressures can be determined using the ideal gas law as follows:

$$p_1 = \frac{m_1 R T_1}{V_1} \,, \tag{32}$$

$$p_2 = \frac{m_2 R T_2}{V_2} \,, \tag{33}$$

and

$$p_3 = \frac{m_3 R T_3}{V_3} \,. \tag{34}$$

5.3 BALANCE OF THE MAGNET VALVE BODY

Since magnet valve is not excited and having $x_{MV\,\max}$ stroke, the stroke limiting force is:

$$F_{MV\,\lim} = 0 \tag{35}$$

The magnetic excitation is:

$$\Theta = N\,I \tag{36}$$

The magnetic flux is defined by the magnetic version of Ohm's law:

$$\Phi = \frac{\Theta}{R_\Sigma} \tag{37}$$

So the magnetic energy of the solenoid valve is:

$$E_{MV} = \frac{\Theta^2}{2R_\Sigma} \tag{38}$$

Conservation balance of magnetic field implies the minimum field energy. So the force developed by the magnetic field is as:

$$F_{MV} = -\frac{\partial E_{MV}}{\partial x_{MV}} = \frac{\Theta^2}{2R_\Sigma{}^2}\frac{dR_\Sigma}{dx_{MV}}. \tag{39}$$

The connected magnetic resistances are related to the frame (R_{MF}), the plug (R_{MP}), the valve body (R_{MB}), the air clearance between the overlapping coaxial cylindrical surfaces of the valve body and the frame (R_{MC1}) and resistance in the air clearance between the plug and valve body (R_{MC2}).

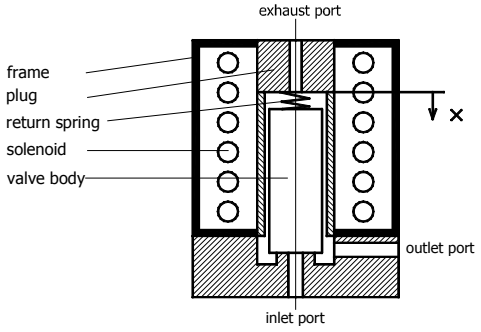

Figure 5 Scheme of the solenoid valve (no excitation)

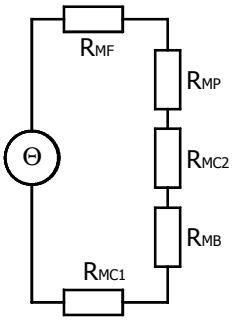

Figure 6 Magnetic circuit of the solenoid valve

The only component that depends in the stroke is R_{MC2}, which is proportional to x_{MV}. R_{MF}, R_{MP}, and R_{MC2} remain unchanged during valve body displacement. The change of R_{MB} is neglectable small so it is considered constant, too.

The magnetic resistance can be calculated as function of magnet valve body stroke from the magnetic circuit shown in Fig. 6. as:

$$R_\Sigma = R_{MP} + R_{MF} + R_{MC1} + R_{MC2} + R_{MB} \tag{40}$$

Since there is only one stroke dependent component, the derivative function with respect to x_{MV} is written as:

$$\frac{dR_\Sigma}{dx_{MV}} = \frac{dR_{MC2}}{dx_{MV}} \tag{41}$$

5.4 AIRFLOW PROPERTIES OF THE MAGNET VALVE

Magnet valve exhaust cross section can be calculated as:

$$A_{MVexh} = \frac{{d_{MVexh}}^2 \pi}{4} \tag{42}$$

Since the inlet port is closed:

$$A_{MVin} = 0\,. \tag{43}$$

According to the magnet valve streaming cross section assumption, control chamber pressure can be used as internal pressure level inside the magnet valve. That means inlet and exhaust sir flows are defined by pressure rate between control chamber pressure and the corresponding port pressures. Furthermore outlet airflow is determined by the following algebraic equation:

$$\mu_{MVout} = \mu_{MVin} - \mu_{MVexh}\,. \tag{44}$$

Exhaust airflow of the magnet valve is written as:

$$\mu_{MVexh} = \alpha_{MV}\, A_{MVexh} \sqrt{2 \frac{\kappa}{\kappa - 1} \frac{p_3\, m_3}{V_3} \left[\left(\frac{p_{env}}{p_3} \right)^{\frac{2}{\kappa}} - \left(\frac{p_{env}}{p_3} \right)^{\frac{\kappa+1}{\kappa}} \right]}\,, \tag{45}$$

and inlet air flow of the magnet valve is:

$$\mu_{MVin} = \alpha_{MV}\, A_{MVin} \sqrt{2 \frac{\kappa}{\kappa - 1} \frac{p_1\, m_1}{V_1} \left[\left(\frac{p_3}{p_1} \right)^{\frac{2}{\kappa}} - \left(\frac{p_3}{p_1} \right)^{\frac{\kappa+1}{\kappa}} \right]}\,. \tag{46}$$

6 HYBRID DOMAINS OF THE MODEL

The above-defined equations describe the system in a special hybrid state only. To generalize the model all of the cases have to be collected that describe the changes in the modelling equations and their domains.

The model includes four general subsystem types that have hybrid behaviour. These are as follows with the included components:

- Gas enthalpies
    - Inlet chamber (4 hybrid-states)
    - Outlet chamber (4 hybrid-states)
    - Control chamber (2 hybrid-states)
- Streaming cross-sections
    - Protection valve (2 hybrid-states)
    - Magnet valve (5 hybrid-states)

- Stroke limiting
    - Protection valve (3 hybrid-states)
    - Magnet valve (3 hybrid-states)
- Air flows and gas speeds
    - Protection valve (5 hybrid-states)
    - Magnet valve (4+2 hybrid-states)

Streaming cross-section and valve stroke limiting subsystems are dependent from each other corresponding the same valve unit, all other are independent. The total number of states is 34.

6.1 GAS ENTHALPIES

In general enthalpies should correspond to gas temperatures wherefrom the gas is coming. Depending on the value of airflow two hybrid states have to be distinguished according to the direction of the flow.

6.1.1 Inlet chamber

Since compressor airflow is assumed to be non-negative, four different cases are obtained.

Inlet chamber Hybrid-State 1: When $\mu_C \geq 0$, $\mu_{PV} \geq 0$, $\mu_{MVin} \geq 0$, Eq. (11) can be written as:

$$\frac{dT_1}{dt} = \kappa \frac{\mu_C T_C - \mu_{PV} T_1 - \mu_{MVin} T_1}{m_1} - \frac{k_1 A_1 (T_1 - T_{env})}{c_v m_1} - \frac{T_1}{m_1}(\mu_C - \mu_{PV} - \mu_{MVin}), \qquad (47)$$

Inlet chamber Hybrid-State 2: When $\mu_C \geq 0$, $\mu_{PV} \geq 0$, $\mu_{MVin} < 0$, Eq. (11) can be written as:

$$\frac{dT_1}{dt} = \kappa \frac{\mu_C T_C - \mu_{PV} T_1 - \mu_{MVin} T_3}{m_1} - \frac{k_1 A_1 (T_1 - T_{env})}{c_v m_1} - \frac{T_1}{m_1}(\mu_C - \mu_{PV} - \mu_{MVin}), \qquad (48)$$

Inlet chamber Hybrid-State 3: When $\mu_C \geq 0$, $\mu_{PV} < 0$, $\mu_{MVin} \geq 0$, Eq. (11) can be written as:

$$\frac{dT_1}{dt} = \kappa \frac{\mu_C T_C - \mu_{PV} T_2 - \mu_{MVin} T_1}{m_1} - \frac{k_1 A_1 (T_1 - T_{env})}{c_v m_1} - \frac{T_1}{m_1}(\mu_C - \mu_{PV} - \mu_{MVin}), \qquad (49)$$

Inlet chamber Hybrid-State 4: When $\mu_C \geq 0$, $\mu_{PV} < 0$, $\mu_{MVin} < 0$, Eq. (11) can be written as:

$$\frac{dT_1}{dt} = \kappa \frac{\mu_C T_C - \mu_{PV} T_2 - \mu_{MVin} T_3}{m_1} - \frac{k_1 A_1 (T_1 - T_{env})}{c_v m_1} - \frac{T_1}{m_1}(\mu_C - \mu_{PV} - \mu_{MVin}), \qquad (50)$$

The state transition graph of the above hybrid states is seen in Fig. 7.

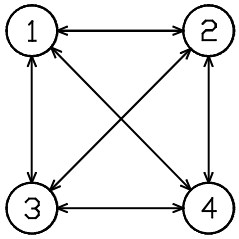

Figure 7 State transition graph for the inlet chamber enthalpies

6.1.2 Outlet chamber

Outlet chamber Hybrid-State 1: When $\mu_{PV} \geq 0$, $\mu_S \geq 0$, Eq. (12) can be written as:

$$\frac{dT_2}{dt} = \kappa \frac{\mu_{PV} T_1 - \mu_S T_2}{m_2} - \frac{k_2 A_2 (T_2 - T_{env})}{c_v m_2} - \frac{T_2}{m_2}(\mu_{PV} - \mu_S). \tag{51}$$

Outlet chamber Hybrid-State 2: When $\mu_{PV} \geq 0$, $\mu_S < 0$, Eq. (12) can be written as:

$$\frac{dT_2}{dt} = \kappa \frac{\mu_{PV} T_1 - \mu_S T_S}{m_2} - \frac{k_2 A_2 (T_2 - T_{env})}{c_v m_2} - \frac{T_2}{m_2}(\mu_{PV} - \mu_S). \tag{52}$$

Outlet chamber Hybrid-State 3: When $\mu_{PV} < 0$, $\mu_S \geq 0$, Eq. (12) can be written as:

$$\frac{dT_2}{dt} = \kappa \frac{\mu_{PV} T_2 - \mu_S T_2}{m_2} - \frac{k_2 A_2 (T_2 - T_{env})}{c_v m_2} - \frac{T_2}{m_2}(\mu_{PV} - \mu_S). \tag{53}$$

Outlet chamber Hybrid-State 4: When $\mu_{PV} < 0$, $\mu_S < 0$, Eq. (12) can be written as:

$$\frac{dT_2}{dt} = \kappa \frac{\mu_{PV} T_2 - \mu_S T_S}{m_2} - \frac{k_2 A_2 (T_2 - T_{env})}{c_v m_2} - \frac{T_2}{m_2}(\mu_{PV} - \mu_S). \tag{54}$$

The state transition graph of the above hybrid states is seen in Fig. 8.

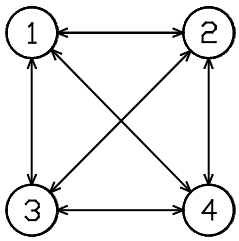

Figure 8 State transition graph for the outlet chamber enthalpies

6.1.3 Control chamber

Control chamber Hybrid-State 1: When $\mu_{MVout} \geq 0$, Eq. (13) can be written as:

$$\frac{dT_3}{dt} = \kappa \frac{\mu_{MVout} T_1}{m_3} - \frac{k_3 A_3 (T_3 - T_{env})}{c_v m_3} - \frac{T_3}{m_3} \mu_{MVout}. \tag{55}$$

Control chamber Hybrid-State 2: When $\mu_{MVout} < 0$, Eq. (13) can be written as:

$$\frac{dT_3}{dt} = \kappa \frac{\mu_{MVout} T_3}{m_3} - \frac{k_3 A_3 (T_3 - T_{env})}{c_v m_3} - \frac{T_3}{m_3} \mu_{MVout}. \tag{56}$$

The state transition graph of the above hybrid states is seen in Fig. 9.

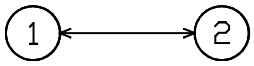

Figure 9 State transition graph for the control chamber enthalpies

6.2 STREAMING CROSS SECTIONS

Streaming cross-sections of valves consider usually cylindrical surface are but they two limits at each sides the one is the closed state and the other is when the cylindrical surface exceeds the circular cross section.

6.2.1 Protection valve

Protection valve streaming cross section Hybrid-State 1: When $x_{PV} < 0$, the cross section of the protection valve given by (29) is:

$$A_{PV} = 0 \tag{57}$$

Protection valve streaming cross section Hybrid-State 2: When $0 \le x_{PV} \le \frac{d_2}{4}$, the cross section of the protection valve given by (29) is:

$$A_{PV} = x d_2 \pi \tag{58}$$

The condition of $x_{PV} > \frac{d_2}{4}$ should be also investigated since the cross section has and upper bound of:

$$A_{PV} = \frac{{d_2}^2 \pi}{4}. \tag{59}$$

But the construction of the investigated protection valve does not allow strokes corresponding this cross section. The state transition graph of the above hybrid states is seen in Fig. 10.

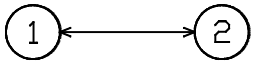

Figure 10 State transition graph for the protection valve streaming cross section

6.2.2 Magnet valve

The magnet valve has two streaming cross-sections that depend on the valve body stroke. The one is on the inlet port the other is on the exhaust port. According to the assumptions concerning magnet valve stroke the following cases are obtained.

Magnet valve streaming cross section Hybrid-State 1: When $x_{MV} < 0$, the streaming cross sections of the magnet valve given by (42) and (43) are:

$$A_{MVexh} = 0 \tag{60}$$

$$A_{MVin} = \frac{{d_{MVin}}^2 \pi}{4} \tag{61}$$

Magnet valve streaming cross section Hybrid-State 2: When $0 \le x_{MV} \le \frac{d_{MVexh}}{4}$, the streaming cross sections of the magnet valve given by (42) and (43) are:

$$A_{MVexh} = x_{MV} d_{MVexh} \pi \tag{62}$$

$$A_{MVin} = \frac{{d_{MVin}}^2 \pi}{4} \tag{63}$$

Magnet valve streaming cross section Hybrid-State 3: When $x_{MV\max} - \frac{d_{MVin}}{4} > x_{MV} > \frac{d_{MVexh}}{4}$, the streaming cross sections of the magnet valve given by (42) and (43) are:

$$A_{MVexh} = \frac{{d_{MVexh}}^2 \pi}{4} \tag{64}$$

$$A_{MVin} = \frac{{d_{MVin}}^2 \pi}{4} \tag{65}$$

Magnet valve streaming cross section Hybrid-State 4: When $x_{MV\max} - \frac{d_{MVin}}{4} \le x_{MV} \le x_{MV\max}$, the streaming cross sections of the magnet valve given by (42) and (43) are:

$$A_{MVexh} = \frac{{d_{MVexh}}^2 \pi}{4} \tag{66}$$

$$A_{MVin} = (x_{MV\max} - x_{MV}) d_{MVin} \pi \tag{67}$$

Magnet valve streaming cross section Hybrid-State 5: When $x_{MV} > x_{MV\max}$, the streaming cross sections of the magnet valve given by (42) and (43) are:

$$A_{MVexh} = \frac{{d_{MVexh}}^2 \pi}{4} \tag{68}$$

$$A_{MVin} = 0 \tag{69}$$

The state transition graph of the above hybrid states is seen in Fig. 11.

Figure 11 State transition graph for the magnet valve streaming cross section

6.3 VALVE BODY STROKES

Valve strokes have two limits at each side according to their physical limits. Strokes exceeding the limiting consider a stiff spring representing the limiting wall. Using this manner the problem remains

an index-1 problem and manageable by ODE solvers. Other opportunity can be simply limiting the stroke values and clearing the valve body speeds, but this case bring a high-index problem because of the imposed algebraic conditions on the differential variables. That would require a special solver that can handle high index problem, so this second case is rejected.

6.3.1 Protection valve

Protection valve limiting force Hybrid-State 1: When $x_{PV} < 0$, the limiting force of the protection valve given by (28) is:

$$F_{PV\lim} = -c_{PV\lim} x_{PV} \tag{70}$$

Protection valve limiting force Hybrid-State 2: When $0 \le x_{PV} \le x_{PV\max}$, the limiting force of the protection valve given by (28) is:

$$F_{PV\lim} = 0 \tag{71}$$

Protection valve limiting force Hybrid-State 3: When $x_{PV} > x_{PV\max}$, the limiting force of the protection valve given by (28) is:

$$F_{PV\lim} = -c_{PV\lim}\left(x_{PV} - x_{PV\max}\right) \tag{72}$$

The state transition graph of the above hybrid states is seen in Fig. 12.

Figure 12 State transition graph for the protection valve stoke limiting

6.3.2 Magnet valve

Magnet valve limiting force Hybrid-State 1: When $x_{MV} < 0$, the limiting force of the magnet valve given by (35) is:

$$F_{MV\lim} = -c_{MV\lim} x_{MV} \tag{73}$$

Magnet valve limiting force Hybrid-State 2: When $0 \le x_{MV} \le x_{MV\max}$, the limiting force of the magnet valve given by (35) is:

$$F_{MV\lim} = 0 \tag{74}$$

Magnet valve limiting force Hybrid-State 3: When $x_{MV} > x_{MV\max}$, the limiting force of the magnet valve given by (35) is:

$$F_{MV\lim} = -c_{MV\lim}\left(x_{MV} - x_{MV\max}\right) \tag{75}$$

The state transition graph of the above hybrid states is seen in Fig. 13.

Figure 13 State transition graph for the magnet valve stoke limiting

6.4 AIR FLOWS AND GAS SPEEDS

Air flows and gas speeds consider value of pressure rates and four cases can be distinguished that can be subsonic and sonic in both directions. The sonic streaming conditions are determined by the critical pressure ratio, which can be written as:

$$\Pi_{critical} = \left(\frac{2}{\kappa+1}\right)^{\frac{\kappa}{\kappa-1}}. \tag{76}$$

6.4.1 Protection valve

Protection valve airflow Hybrid-State 1: When $1 \geq \frac{p_2}{p_1} > \Pi_{crit}$ and $x_{PV} > 0$:

The local speed at *vena contracta* given by (30):

$$s_{PV} = \sqrt{2\frac{\kappa}{\kappa-1}RT_1\left[1-\left(\frac{p_2}{p_1}\right)^{\frac{\kappa-1}{\kappa}}\right]}, \tag{77}$$

The airflow through the protection valve given by (31) is:

$$\mu_{PV} = \alpha_{PV} A_{PV}\sqrt{2\frac{\kappa}{\kappa-1}\frac{p_1 m_1}{V_1}\left[\left(\frac{p_2}{p_1}\right)^{\frac{2}{\kappa}}-\left(\frac{p_2}{p_1}\right)^{\frac{\kappa+1}{\kappa}}\right]} \tag{78}$$

Protection valve airflow Hybrid-State 2: When $\frac{p_2}{p_1} \leq \Pi_{crit}$ and $x_{PV} > 0$:

The local speed at *vena contracta* given by (30):

$$s_{PV} = \sqrt{2\frac{\kappa}{\kappa-1}RT_1\left[1-\Pi_{crit}^{\frac{\kappa-1}{\kappa}}\right]}, \tag{79}$$

The airflow through the protection valve given by (31) is:

$$\mu_{PV} = \alpha_{PV} A_{PV}\sqrt{2\frac{\kappa}{\kappa-1}\frac{p_1 m_1}{V_1}\left[\Pi_{crit}^{\frac{2}{\kappa}}-\Pi_{crit}^{\frac{\kappa+1}{\kappa}}\right]} \tag{80}$$

Protection valve airflow Hybrid-State 3: When $1 > \frac{p_1}{p_2} > \Pi_{crit}$ and $x_{PV} > 0$:

The local speed at *vena contracta* given by (30):

$$s_{PV} = -\sqrt{2\frac{\kappa}{\kappa-1}RT_2\left[1-\left(\frac{p_1}{p_2}\right)^{\frac{\kappa-1}{\kappa}}\right]}, \tag{81}$$

The airflow through the protection valve given by (31) is:

$$\mu_{PV} = -\alpha_{PV} A_{PV} \sqrt{2 \frac{\kappa}{\kappa - 1} \frac{p_2 m_2}{V_2} \left[\left(\frac{p_1}{p_2} \right)^{\frac{2}{\kappa}} - \left(\frac{p_1}{p_2} \right)^{\frac{\kappa+1}{\kappa}} \right]} \tag{82}$$

Protection valve airflow Hybrid-State 4: When $\frac{p_1}{p_2} \leq \Pi_{crit}$ and $x_{PV} > 0$:

The local speed at *vena contracta* given by (30):

$$s_{PV} = -\sqrt{2 \frac{\kappa}{\kappa - 1} R T_2 \left[1 - \Pi_{crit}^{\frac{\kappa-1}{\kappa}} \right]}, \tag{83}$$

The airflow through the protection valve given by (31) is:

$$\mu_{PV} = -\alpha_{PV} A_{PV} \sqrt{2 \frac{\kappa}{\kappa - 1} \frac{p_2 m_2}{V_2} \left[\Pi_{crit}^{\frac{2}{\kappa}} - \Pi_{crit}^{\frac{\kappa+1}{\kappa}} \right]} \tag{84}$$

Protection valve airflow Hybrid-State 5: When $x_{PV} \leq 0$:

The local speed at *vena contracta* given by (30):

$$s_{PV} = 0, \tag{85}$$

The airflow through the protection valve given by (31) is:

$$\mu_{PV} = 0, \tag{86}$$

since the streaming cross section is zero. The state transition graph of the above hybrid states is seen in Fig. 14.

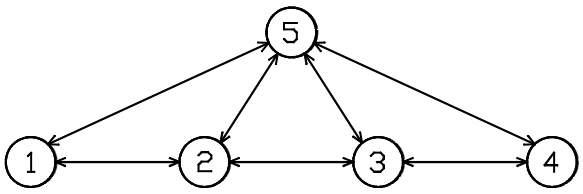

Figure 14 State transition graph for the protection valve stoke limiting

6.4.2 Magnet valve

According to the magnet valve streaming cross section assumption control chamber pressure can be used as internal pressure level inside the magnet valve. That is, two independent cases are obtained the one is for inlet airflow and the other is for the exhaust one.

6.4.2.1 Inlet air flow

Magnet valve inlet airflow Hybrid-State 1: When $1 \geq \frac{p_3}{p_1} > \Pi_{crit}$, the inlet airflow of the magnet valve given by (46) is:

$$\mu_{MVin} = \alpha_{MV} A_{MVin} \sqrt{2 \frac{\kappa}{\kappa - 1} \frac{p_1 m_1}{V_1} \left[\left(\frac{p_3}{p_1} \right)^{\frac{2}{\kappa}} - \left(\frac{p_3}{p_1} \right)^{\frac{\kappa+1}{\kappa}} \right]}. \quad (87)$$

Magnet valve inlet airflow Hybrid-State 2: When $\frac{p_3}{p_1} \leq \Pi_{crit}$, the inlet airflow of the magnet valve given by (46) is:

$$\mu_{MVin} = \alpha_{MV} A_{MVin} \sqrt{2 \frac{\kappa}{\kappa - 1} \frac{p_1 m_1}{V_1} \left[\Pi_{crit}^{\frac{2}{\kappa}} - \Pi_{crit}^{\frac{\kappa+1}{\kappa}} \right]} \quad (88)$$

Magnet valve inlet airflow Hybrid-State 3: When $1 > \frac{p_1}{p_3} > \Pi_{crit}$, the inlet airflow of the magnet valve given by (46) is:

$$\mu_{MVin} = -\alpha_{MV} A_{MVin} \sqrt{2 \frac{\kappa}{\kappa - 1} \frac{p_3 m_3}{V_3} \left[\left(\frac{p_1}{p_3} \right)^{\frac{2}{\kappa}} - \left(\frac{p_1}{p_3} \right)^{\frac{\kappa+1}{\kappa}} \right]}. \quad (89)$$

Magnet valve inlet airflow Hybrid-State 4: When $\frac{p_1}{p_3} \leq \Pi_{crit}$, the inlet airflow of the magnet valve given by (46) is:

$$\mu_{MVin} = -\alpha_{MV} A_{MVin} \sqrt{2 \frac{\kappa}{\kappa - 1} \frac{p_3 m_3}{V_3} \left[\Pi_{crit}^{\frac{2}{\kappa}} - \Pi_{crit}^{\frac{\kappa+1}{\kappa}} \right]} \quad (90)$$

The state transition graph of the above hybrid states is seen in Fig. 15.

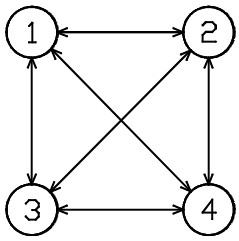

Figure 15 State transition graph for the magnet valve inlet air flow

6.4.2.2 Exhaust air flow

Magnet valve exhaust airflow Hybrid-State 1: When $1 \geq \frac{p_{env}}{p_3} > \Pi_{crit}$, the exhaust airflow of the magnet valve given by (45) is:

$$\mu_{MVexh} = \alpha_{MV} A_{MVexh} \sqrt{2 \frac{\kappa}{\kappa - 1} \frac{p_3 m_3}{V_3} \left[\left(\frac{p_{env}}{p_3} \right)^{\frac{2}{\kappa}} - \left(\frac{p_{env}}{p_3} \right)^{\frac{\kappa+1}{\kappa}} \right]}, \quad (91)$$

Magnet valve exhaust airflow Hybrid-State 2: When $\frac{p_{env}}{p_3} \leq \Pi_{crit}$, the exhaust airflow of the magnet valve given by (45) is:

$$\mu_{MVexh} = \alpha_{MV} A_{MVexh} \sqrt{2 \frac{\kappa}{\kappa - 1} \frac{p_3 m_3}{V_3} \left[\Pi_{crit}^{\frac{2}{\kappa}} - \Pi_{crit}^{\frac{\kappa+1}{\kappa}} \right]}, \tag{92}$$

The state transition graph of the above hybrid states is seen in Fig. 16.

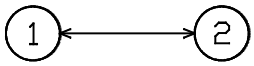

Figure 16 State transition graph for the magnet valve exhaust air flow

7 VARIABLES

7.1 STATE VECTOR OF THE NONLINEAR MODEL

$$\underline{q} = \begin{bmatrix} m_1 & T_1 & m_2 & T_2 & m_3 & T_3 & x & \dot{x} & x_{MV} & \dot{x}_{MV} & I \end{bmatrix}^T \tag{93}$$

7.2 DISTURBANCE VECTOR

$$\underline{d} = \begin{bmatrix} \mu_C & T_C & \mu_S & T_S & T_{env} & p_{env} \end{bmatrix}^T \tag{94}$$

The included two airflows are not measurable only calculable. μ_C airflow can be calculated (estimated) from the current charge of compressor. Output μ_S airflow can be obtained by brake system and other system intervention's (e.g. levelling control and booster activity) air consumption based on driving situation.

The brake system's air consumption calculation should be based on fill processes of brake chambers by wheel modules (in case of Electro-pneumatic brake system - EBS) or pedal valve (in case of conventional one).

This air consumption is very dominant in case of anti-lock braking or anti skid control's intervention having frequent fill-hold-exhaust cycles of wheel brake chambers.

7.3 INPUT VECTOR

The input vector includes one member only, which is the excitation voltage of the magnet valve so:

$$\underline{u} = \begin{bmatrix} U \end{bmatrix} \tag{95}$$

7.4 MEASURED OUTPUT

The measured output includes the chamber pressures as:

$$\underline{y} = \begin{bmatrix} p_1 & p_2 & p_3 \end{bmatrix}^T \tag{96}$$

7.5 PERFORMACE OUTPUT

The performance output is the outlet chamber pressure as:

$$\underline{z} = [p_2] \tag{97}$$

7.6 OPERATING RANGE

The following operation domain can be investigated on test-bench concerning the state vector (93) members:

$0.0001 \le m_1 \le 0.2$, $0.001 \le m_2 \le 0.4$, $0.00001 \le m_3 \le 0.01$,

$203.15 \le T_1 \le 403.15$, $203.15 \le T_2 \le 403.15$, $203.15 \le T_3 \le 403.15$,

$-0.0001 \le x_{PV} \le 0.0003$, $-50 \le \dot{x}_{PV} \le 50$, $-0.00001 \le x_{MV} \le 0.0001$,

$-0.00001 \le x_{MV} \le 0.0001$ $-50 \le \dot{x}_{MV} \le 50$ $0 \le I \le 1$

The values of the input variable is constrained as:

$$0 \le U \le 30$$

The values of the measured and performance output members are limited as:

$100000 \le p_1 \le 1600000$, $100000 \le p_2 \le 1600000$, $100000 \le p_3 \le 1600000$

8 MODEL ANALYSIS

8.1 DIFFERENTIAL AND ALGEBRAIC VARIABLES

The differential variables are: m_1, T_1, m_2, T_2, m_3, T_3, x_{PV}, $\dot{x}_{PV}$, x_{MV}, $\dot{x}_{MV}$, I.

The algebraic variables are as follows: μ_C, μ_{PV}, μ_{MVin}, μ_{MVout}, μ_{MVexh}, μ_S, p_{env}, T_{env}, T_C, T_S, p_1, p_2, p_2, F_{PV1}, F_{PV2}, $F_{PV\,\mathrm{lim}}$, F_{MV}, $F_{MV\,\mathrm{lim}}$, L, R_Σ, φ, A_{PV}, c_{PV}, A_{MVexh}, A_{MVin}, Θ, $\frac{dR_\Sigma}{dx_{MV}}$.

Number of differential variables: $N_d = 11$.

Number of algebraic variables: $N_a = 27$.

Number of unknowns (variables): $N_u = N_d + N_a = 38$.

Number of equations: $N_e = 11 + 21 = 32$.

The model parameters can be seen in Tab. 1.

8.2 DEGREE OF FREEDOM

Since the model has many hybrid states the degree of freedom is also depending on the corresponding states the system is working in. The analysis shows that the maximal degree of freedom is 6, since: $N_{DF} = N_u - N_e = 6$. The free variables refer to the components of the disturbance vector. The minimal degree of freedom is 3. In this case the free variables are: μ_C, μ_S and T_{env}, where the airflow variables cannot be measured. Depending on the values of system inlet-, outlet airflows and the magnet valve body position the degree of freedom can vary between these minimum and maximum values.

8.3 INPUT AFFINITY

The model is termed input affine since the state equations include the input signal as linear expression.

8.4 SUBSTITUTABILITY

The model is substitutable because all constitutive (algebraic) equations in all hybrid states can be substituted into the state equations producing a set of ODE systems.

8.5 SYSTEM INDEX

The built up model is termed index-1 system, that is, the algebraic system of equations undergo to convert the system into a set of ODEs after one differentiation step with respect to time.

9 MODEL VERIFICATION

The verification of the developed non-linear model is performed by extensive simulation experiments using MATLAB/SIMULINK model against engineering intuition and operation experience on the quantitative behaviour of the system. Parameters considered in simulation calculations can be seen in Tab.1.

From the above parameters the following items have to be identified: α_{PV}, α_{MV}, V_1, V_2, V_3, k_1, k_2, k_3, A_1, A_2, A_3, R_{MF}, R_{MP}, R_{MB}, R_{MC10}, R_{MC2}, a_1 and a_2.

Table 1 Parameters of the simulation model

Parameter	Symbol	Unit	Value
Contraction coefficient	α_{PV}	-	0.8
Pressure distribution param1	a_1	rad	0
Pressure distribution param2	a_2	rad s/m	0.002
Outer diameter of protection valve piston	d_1	m	0.022
Valve seat diameter of protection valve	d_2	m	0.013
Maximal piston stroke	x_{PVmax}	m	0.0025
Spring preset yield stroke	x_{PV0}	m	0.004
Stiffness of spring	c_{PV}	N/m	40000
Mass of piston	m_{PV}	kg	0.02
Input chamber volume	V_1	m^3	0.001
Output chamber volume	V_2	m^3	0.02
Control chamber volume	V_3	m^3	0.00005
Input chamber surface area	A_1	m^2	0.01
Output chamber surface area	A_2	m^2	0.1
Output chamber surface area	A_3	m^2	0.001
Input chamber's heat transfer coefficient	k_1	W/m^2K	100
Output chamber's heat transfer coefficient	k_2	W/m^2K	100
Output chamber's heat transfer coefficient	k_3	W/m^2K	100
MV contraction coefficient	α_{MV}	-	0.7
Magnet valve inlet diameter	d_{MVin}	m	0.0009
Magnet valve outlet diameter	d_{MVout}	m	0.003
Magnet valve exhaust diameter	d_{MVexh}	m	0.0009
Magnet valve body diameter	d_{MV}	m	0.008
Maximal magnet valve stroke	x_{MVmax}	m	0.0008
Magnetic resistance of plug part	R_{MP}	A/Vs	1e4
Magnetic resistance of magnet valve body	R_{MB}	A/Vs	1e6
Magnetic resistance of magnet valve frame	R_{MF}	A/Vs	1e6
Magnetic resistance of air clearance1	R_{MC10}	A/Vs	1e9
Magnetic resistance of air clearance2	R_{MC2}	A/Vs	1e9
Number of magnet valve turns	N	-	1320
Electric resistance of magnet valve	R	Ohm	31.5
Spring preset yield stroke of MV	x_{MV0}	m	0.0025
Stiffness of spring of MV	c_{MV}	N/m	1000
Stiffness of limiting spring of PV	c_{PVlim}	N/m	1e7
Stiffness of limiting spring of MV	c_{MVlim}	N/m	1e7
Damping coefficient of PV	k_{PV}	Ns/m	5
Damping coefficient of MV	k_{MV}	Ns/m	1

9.1 SIMULATION RESULTS

The simulation calculations considered two typical operating situations without modulation of magnet valve since the experiences with conventional systems refer to protection valve behaviour without magnet valve (open-loop properties). So the used input vector is as:

$$\underline{u} = [0]$$

The responses corresponded to the engineering expectations: in fill up case inlet chamber pressure increased, after reaching dynamic opening pressure of the protection valve the valve stroke increases and as effect the outlet chamber pressure increased. In circuit defect case inlet and outlet chamber pressures decreased, on reaching the dynamic closing pressure of the protection valve the valve stroke decreases and finally it closed so the inlet chamber pressure is protected against the circuit defect.

9.1.1 Fill up process

This case is simulated with constant compressor fill airflow and constant filling gas temperature (accomplished by intercooling). The initial state vector is as follows:

$$\underline{q}^* = [0.0011892 \quad 293.15 \quad 0.023784 \quad 293.15 \quad 0.0000059446 \quad 293.15 \quad 0 \quad 0 \quad 0 \quad 0 \quad 0]^T$$

The disturbance vector is considered as:

$$\underline{d}^* = [0.01 \quad 293.15 \quad 0 \quad 293.15 \quad 293.15 \quad 100000]^T$$

The dynamic response functions are shown in the Appendix. (See Fig. 7)

9.1.2 Circuit defect situation

This case was simulated with 5 mm diameter leakage of circuit to the 10^5 Pa environment starting from the common 10^6 Pa pressure level. No input side airflow was considered.
The initial state vector is as follows:

$$\underline{q}^* = [0.011892 \quad 293.15 \quad 0.23784 \quad 293.15 \quad 0.0000059446 \quad 293.15 \quad 0.025 \quad 0 \quad 0 \quad 0 \quad 0]^T$$

The initial disturbance vector is considered as:

$$\underline{d}^* = [0 \quad 293.15 \quad 0 \quad 293.15 \quad 293.15 \quad 100000]^T$$

The dynamic response functions are shown in the Appendix. (See Fig. 8).

10 CONCLUSIONS AND FUTURE WORK

A nonlinear hybrid model of a single protection valve has been developed using fluid-, thermo- and magneto-dynamic considerations, being capable for prediction on dynamic behaviour of the real system, as well as selected a model instance for verification purposes. The model has been analysed from computational point of view and verified in two cases against engineering intuition.

For future work the following items are foreseen:

- Model simplification
- Verification of simplified model
- Parameter sensitivity analysis
- Model parameter estimation

11 REFERENCES

[1] Ailer, P., Sánta, I., Szederkényi, G. and Hangos, K. M. (2001) *Nonlinear Model-building of a Low-Power Gas Turbine.* Periodica Polytechnica, published by the Budapest University of Technology and Economics.

[2] Ailer, P., Szederkényi, G. and Hangos, K. M. (2001) *Modelling and Nonlinear Analysis of a Low-Power Gas Turbine.* Research Report of Computer and Automation Research Institute, **SCL-1/2001**

[3] Hangos, K. M. and Cameron, I. (2001) *Process Modelling and Model Analysis.* Process systems engineering Volume 4, Academic Press, London.

[4] Hős, Cs., Istók, B., Szente, V., Kristóf, G., and Vad, J. (2000) *Pneumatic Pipe Models Adapted to an Advanced Environment for Simulating Engineering Systems.* Periodica Polytechnica, Mechanical engineering Series. A contribution to international technical sciences, published by the Budapest University of Technology and Economics.

[5] Ljung L. and T. Glad. (1994) *Modeling of Dynamic Systems*, Prentice Hall, Englewood Cliffs, N.J.

[6] Oppenheim J. and A.S. Willsky. (1985) *Signals and Systems*, Prentice Hall, Englewood Cliffs, N.J.

[7] Pásztor E., Konecsny F., Benedek Z., Hatházi D., Kiss E., Perjési I., Sánta I., Steiger I. (1993). *Műszaki hő- és áramlástan I/1, I/2, II.* (Engineering thermo- and fluid dynamics) Műegyetemi Kiadó, Budapest.

[8] Szente, V., Vad, J., Lóránt, G., Fries, A. (2001) *Computational and Experimental Investigation on Dynamics of Electric Braking Systems*, Proc. 7th Scandinavian International Conference on Fluid Power, May 2001, Linköping, Sweden, Vol. I, pp. 263 - 75.

[9] Szente, V., Vad, J. (2001) *Computational and Experimental Investigation on Solenoid Valve Dynamics*, Proc. 2001 IEEE/ASME International Conference on Advanced Intelligent Mechatronics, July 2001, Como, Italy, Vol. I., pp. 618 - 623.

APPENDIX

NOMENCLATURE

	Variables
c	specific heat [J/kgK]
	spring coefficient [N/m]
s	gas speed [m/s]
i	enthalpy [J/kgK]
p	absolute pressure [Pa]
m	mass [kg]
x	stroke [m]
t	time [s]
Q	heat [J]
R	specific gas constant [J/kgK],
	resistance [electric-Ω; magnetic-A/Vs]
U	internal energy [J]
	voltage [V]
V	volume [m^3]
κ	adiabatic exponent [-]
I	electric current [A]
F	force [N]
Θ	magnetic excitation [I]
Φ	magnetic flux [Vs]
L	inductance [Vs/A]
T	absolute temperature [K]
A	area, surface [m^2]
d	diameter [m]
φ	angle [-]
k	coefficient of heat transmission [W/m^2K]
	damping coefficient [Ns/m]
a	pressure distribution factor [-;s/m]
α	contraction coefficient [-]
Π	pressure ratio [-]
E	energy [J]
N	solenoid turns [-]
μ	air flow [kg/s]
v	speed [m/s]
h	length [m]

	Indices
0	refers to initial state
1	refers to input chamber
2	refers to output chamber
3	refers to control chamber
PV	refers to protection valve
C	refers to compressor
Σ	refers to magnetic resultant
v	refers to constant volume
p	refers to constant pressure
MV	refers to magnet valve
env	refers to environment
S	refers to brake system
MF	refers to magnet valve frame
MJ	refers to magnet valve jacket
MB	refers to magnet valve body
MC1	refers to magnet valve clearance 1
MC2	refers to magnet valve clearance 2
in	refers to inlet
out	refers to outlet
exh	refers to exhaust

FIGURES OF SIMULATION RESULTS

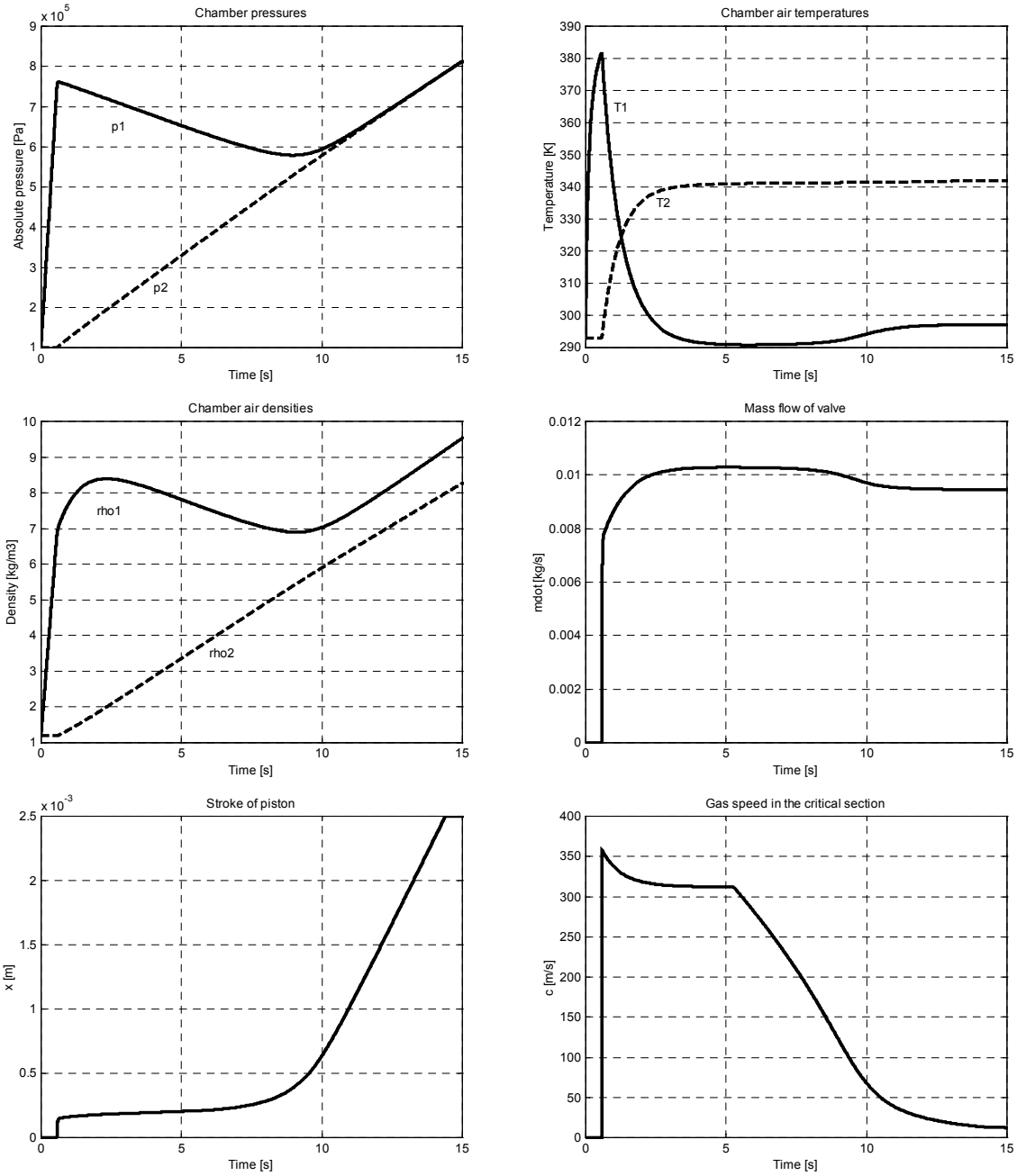

Figure 7 Circuit fill up process

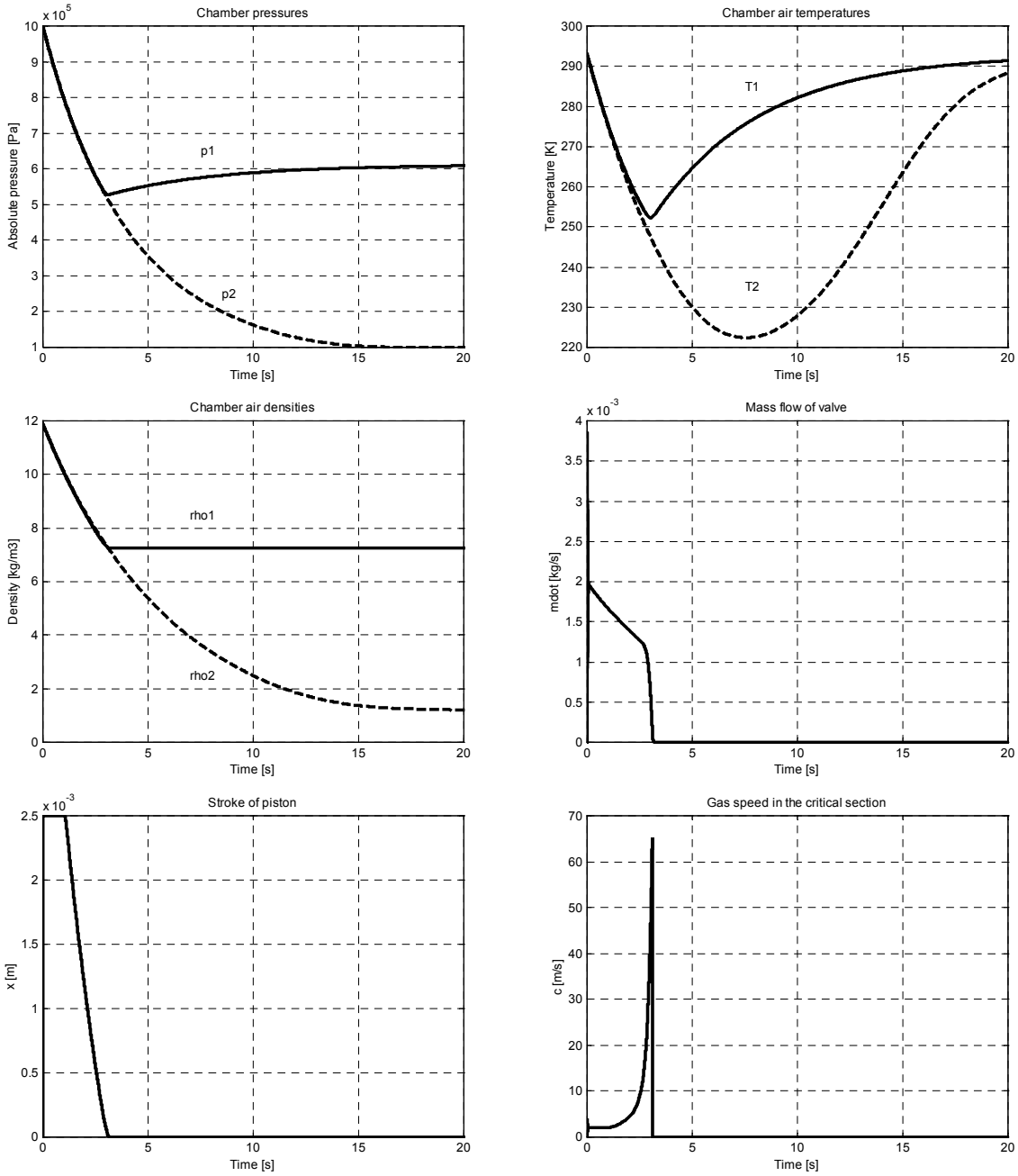

Figure 8 Circuit defect situation